*URSI GASS 2020, Rome, Italy, 29 August - 5 September 2020*

# Investigation of Accelerated Monostatic Radar Cross Section Computations by Using Block and Projection Iterative Methods

Daniel Ostrzyharczik, Thomas F. Eibert
Chair of High-Frequency Engineering
Department of Electrical and Computer Engineering
Technical University of Munich
80290 Munich, Germany

## Abstract

Accurate numerical solutions of scattering phenomena can be achieved by method of moments (MoM) solutions of integral equations. For the evaluation of the monostatic radar cross section (RCS) of an object, the same system of equations has to be solved many times for different excitation fields incident from many directions. Especially for electrically large bodies involving many millions of unknowns, this becomes computationally demanding. In this work, we study and compare the performance of block and projection iterative methods for MoM solutions of surface integral equations related to perfect electrically conducting objects. Both methods are capable of reducing the overall number of matrix-vector products in the considered iterative solution process.

## 1 Introduction

Monostatic RCS computations play an important role in many modern electromagnetic design processes. An accurate numerical representation of the physical scattering phenomena of PEC objects is provided by MoM solutions of surface integral equations [1].
Electrically large objects can lead to systems of equations with many millions of unknowns, thus, rendering such full-wave methods computationally very demanding. Over the last decades, a variety of methods have been proposed to tackle this problem. These methods can be divided into two main categories, namely direct and iterative methods [2].
Direct methods aim at computing an explicit inverse of the matrix of the linear system of equations, which arises in the discretization process of an integral equation. Classical approaches compute the inverse via the Gaussian elimination or the $LU$-decomposition, whose computational and storage complexities scale with $\mathcal{O}(N^3)$ and $\mathcal{O}(N^2)$, respectively, where $N$ refers to the number of unknowns. Especially for large structures, computations with those methods become too cumbersome. For this reason, accelerated techniques have been designed, which construct a low-rank approximation for the inverse of the system matrix, e.g., see [3].
Iterative methods avoid the explicit inversion of the system matrix by consecutively performing matrix-vector products, in order to generate a search space, in which an approximate solution is found. This process is repeated until a certain error criterion is met.
The main issue in computing the monostatic RCS of an object is the fact that the linear system of equations has to be solved all over again, whenever the incident direction of the electromagnetic wave is changed, i.e., for every single monostatic observation direction.
It is possible to directly invoke all incident wave for all incident directions as a collection of right-hand sides (RHSs) in the solution process. This is achieved by so-called block methods, which are augmented versions of the classic iterative methods [4]. The expanded search space, in which the overall solution is found, helps to improve the convergence of the overall solution process, thus, leading to fewer overall matrix-vector products and, in turn, also to less computation time. The expanded search space leads to an increase in storage requirements, which can be a problem for the computation of large objects with many RHSs. This can be remedied by using projection methods [5], which treat only one RHS at a time, but generate a new initial solution by utilizing previously obtained solutions for different incident directions. The new initial solution may lead to a lower initial residual, such that fewer iteration steps are needed in order to meet the error criterion.
In this study, we work with an augmented version of the Flexible Generalized Minimal Residual Method (FGMRES) [6], the Block FGMRES (BFGMRES), and compare it to Galerkin projection methods (GPMs) as well as to the standard FGMRES.

## 2 Problem Statement

A scattering object is characterized by its radar-cross-section (RCS), which is given as

$$\sigma(\vartheta_s, \varphi_s, \vartheta_i, \varphi_i) = \lim_{r\longrightarrow\infty} 4\pi r^2 \frac{|\boldsymbol{E}^{\mathrm{sca}}(\vartheta_s, \varphi_s)|^2}{|\boldsymbol{E}^{\mathrm{inc}}(\vartheta_i, \varphi_i)|^2} \quad (1)$$

with scattered electric field $\boldsymbol{E}^{\mathrm{sca}}$ for the scattering angles $\vartheta_s, \varphi_s$, for an incident plane wave with electric field $\boldsymbol{E}^{\mathrm{inc}}$ with incident angles $\vartheta_i, \varphi_i$. A suppressed time factor

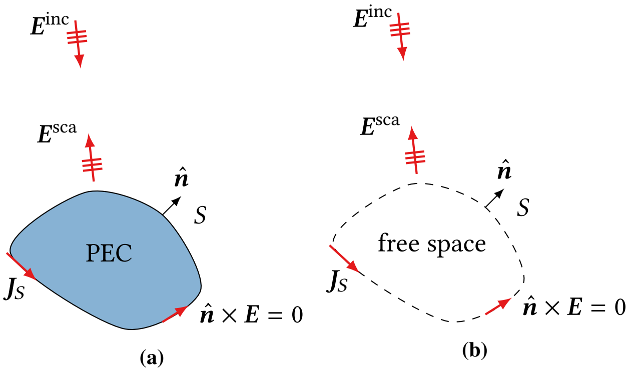


**Figure 1.** Scattering scenario for the monostatic RCS. (a) A PEC object generates a scattered electric field. (b) Equivalent formulation via the Huygens Principle, where the scattered field is produced by the equivalent Huygens surface current densities.

$e^{j\omega t}$ dependent on the angular frequency $\omega$ is considered throughout this paper. Consider the monostatic case of the RCS of an object with $\vartheta_s = \vartheta_i$ and $\varphi_s = \varphi_i$ and a scattering configuration with a perfect electrically conducting (PEC) object as depicted in Fig. 1. The incident field $\boldsymbol{E}^{\mathrm{inc}}$ causes a scattered field together with surface current densities $\boldsymbol{J}_S$ on the object. According to the Huygens principle [7], the surface current densities produce the scattered fields $\boldsymbol{E}^{\mathrm{sca}}$ after the PEC object has been removed, see the equivalent configuration in Fig. 1(b). By enforcing the boundary condition of the total electric field

$$\hat{\boldsymbol{n}} \times \boldsymbol{E} = \hat{\boldsymbol{n}} \times \left( \boldsymbol{E}^{\mathrm{inc}} + \boldsymbol{E}^{\mathrm{sca}}(\boldsymbol{J}_s) \right) = 0 \qquad (2)$$

on the surface of the object, the electric field integral equation (EFIE) for the determination of the unknown surface current densities is obtained [1]. The unit normal vector $\hat{\boldsymbol{n}}$ points from the surface $S$ into the solution domain. By looking at the boundary condition for the total magnetic field $\boldsymbol{H}$, another surface integral equation, the magnetic field integral equation (MFIE), can be derived [2]. In order to avoid parasitic numerical resonances during the solution process of the integral equations, it is common to work with the combined field integral equation (CFIE) according to

$$Z_0(1-\alpha)\,\mathrm{MFIE} - \alpha\,\mathrm{EFIE} = 0 \text{ with } \alpha \in [0,1]\,, \qquad (3)$$

if closed scattering objects need to be handled. $Z_0$ is here the impedance of free space and $\alpha$ the combination parameter leading to the designation CFIE-$\alpha$ [2].

## 3 MoM Formulation

The MoM is used in order to discretize the considered surface integral equation. This leads to a system of equations in the form

$$\boldsymbol{A}\boldsymbol{x} = \boldsymbol{b}, \qquad (4)$$

where $\boldsymbol{A} \in \mathbb{C}^{N\times N}$ is the MoM matrix containing the complex elements of the discretized integral operator with $N$ unknowns, $\boldsymbol{x} \in \mathbb{C}^{N\times 1}$ is the solution vector, and $\boldsymbol{b} \in \mathbb{C}^{N\times 1}$ is the excitation vector, which represents the incident field.

In order to determine the monostatic RCS for varying incident angles $\vartheta_i, \varphi_i$, the same linear system of equations has to be solved all over again, since an incident field with varying angles $\vartheta_i, \varphi_i$ results in new RHS vectors $\boldsymbol{b}$. The RHS vectors can be collected in a matrix and the corresponding system of equations can be written in the form

$$\boldsymbol{A}\boldsymbol{X} = \boldsymbol{B}, \qquad (5)$$

where $\boldsymbol{X} = [\boldsymbol{x}_1, \ldots, \boldsymbol{x}_s] \in \mathbb{C}^{N\times s}$ is a collection of $s$ solution vectors and $\boldsymbol{B} = [\boldsymbol{b}_1, \ldots, \boldsymbol{b}_s] \in \mathbb{C}^{N\times s}$ is a collection of $s$ excitation vectors [4].

### 3.1 Block Flexible Generalized Minimal Residual Method (BFGMRES)

The BFGMRES is an augmented version of the FGMRES [6], which is capable of treating multiple RHS in one solution process. The BFGMRES allows for varying preconditioners, which can be used in an iterative manner [8]. The BFGMRES uses all given RHSs simultaneously for the generation of an extended search space [9]. This block search space is spanned by all given RHSs, making it much larger than the search space, which is spanned by only one RHS. Hence, every individual solution is found in a larger search space, which may result in a better convergence behavior of the solution process. The reason for the improved convergence is that the individual solutions can share certain commonalities among each other, thus, making it beneficial to search the approximative solution in an extended search space. The storage complexity for the BFGMRES rises roughly with a factor of $s$, with $s$ indicating the number of RHSs.

### 3.2 Projection Methods

Projection methods describe techniques, which find an initial solution of an equation systems of the form

$$\boldsymbol{A}\boldsymbol{x}^{(i)} = \boldsymbol{b}^{(i)}, \qquad (6)$$

where $i$ is the index of a RHS, based on previously solved systems with $k = 1, \ldots, i-1$ [5]. The whole solution process can, therefore, be described as a sequence

$$\mathcal{P}_i : \quad \boldsymbol{A}\boldsymbol{x}^{(i)} = \boldsymbol{b}^{(i)} \quad i \in [1, \ldots, ] \qquad (7)$$

of linear systems of equations. Since the success of the projection methods depends on the previously generated solutions, it is required that the solutions share a certain degree of similarity among each other. In the monostatic RCS case, this is accomplished by ensuring that the angular sampling criterion is met, which is required to accurately reconstruct the 3$D$ monostatic RCS [10]. Also, subsequent solutions should work with excitations according to neighboring incident angles on the monostatic RCS sampling grid. Similar requirements should, of course, also be fulfilled for the block of RHSs considered in one BFGMRES solution, as discussed in Section 3.1.

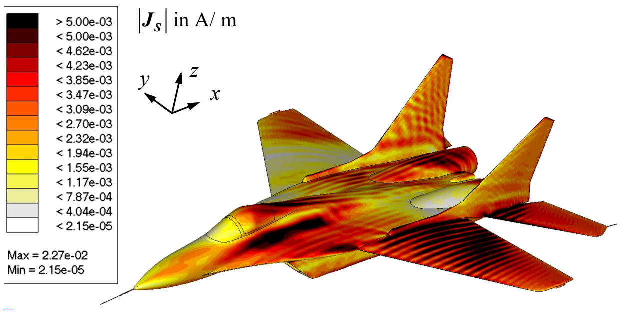


**Figure 2.** Electric surface current density distribution on the MiG-29 model.

The projection methods considered in this study construct a new solution as a weighted sum of $m$ already obtained solutions, whose weighting coefficients are determined via a Galerkin method [11]. The new initial solution can, thus, be written as

$$\boldsymbol{x}_0^{(i)} = \sum_{k=i-m}^{i-1} \boldsymbol{x}^{(k)} \alpha_k, \qquad (8)$$

where the $m$ weighting coefficients $\alpha_k$ are determined with a Galerkin method. Of course, it is also possible to modify the already obtained solutions towards a better performance, before the Galerkin method is employed.

## 4 Numerical Results

We consider the realistic metallic model of a MiG-29 aircraft, which is discretized for $f = 1.5\,\mathrm{GHz}$ with 2 912 091 Rao-Wilton-Glisson (RWG) basis functions. The model, illustrated with an induced surface current density distribution $|J_S|$, is depicted in Fig. 2. The largest extent of the flight object is found in longitudinal direction with a length of 17.5 m. The radius of the enclosing minimum sphere [10] has a value of 8.75 m resulting in a necessary spherical multipole order of $L = 285$ for the expansion of the scattering fields at the frequency $f = 1.5\,\mathrm{GHz}$. The multipole order $L$ determines the minimum required angular sampling distance, in order to correctly reconstruct the 3$D$ RCS. In the monostatic case, the angular sample spacings are obtained as $\Delta\vartheta = \Delta\varphi \approx 0.3^\circ$. Table 1 illustrates the results of the monostatic RCS computations for the combined field integral equation (CFIE-0.9). The solution process has been carried out for 35 RHSs and the solver was restarted after 100 iterations for the BFGMRES and after 400 for the GPM method. The chosen angular step size is $\Delta\vartheta = \Delta\varphi \approx 0.2^\circ$, which is slightly oversampled, in order to guarantee that the solutions share a certain amount of similarity among each other. Both methods are compared to the standard FGMRES. All three solvers worked with an iterative near-zone preconditioner according to the inner/outer iterative solution scheme [8, 11]. The solution process was stopped at a relative residual error of $10^{-4}$ for all solver configurations. The BFGMRES and also the GPM can lead to computation savings of more than 60%, which is especially remarkable for the GPM. Compared to the BFGMRES, the GPM needs considerably less memory due to the considerably smaller search space during the actual system of equations solutions.

| Solver type for CFIE | Average number of iterations |
|---|---|
| BFGMRES, 35 | 242 |
| GPM, 2 | 281 |
| GPM, 3 | 236 |
| GPM, 5 | 276 |
| FGMRES | 691 |

**Table 1.** Average number of iterations for CFIE-0.9 with $f_1 = 1.5\,\mathrm{GHz}$, 2 912 091 RWG unknowns, and a sampling rate of $\Delta\vartheta = \Delta\varphi \approx 0.2^\circ$ (oversampled). The relative residual error was set to $10^{-4}$ as stopping criterion. The BFGMRES and the GPM are compared to the standard FGMRES. The numbers after BFGMRES and GPM indicate how many RHS and previous solutions have been taken into account, respectively. In the case of BFGMRES, deflation reduced the 35 RHSs to 24 before the first restart after 100 iterations, which was considered to correspondingly scale down the number of iterations.

## 5 Conclusion

The block flexible generalized minimal residual (BFGMRES) solver and the Galerkin-based projection methods considered in this work managed both to reduce the overall number of iterations in the monostatic radar cross section solution process of scattering integral equations with multiple incident directions, in comparison to the standard FGMRES solver. Both methods do require a certain similarity between the different considered excitations, which may be achieved by considering neighboring incident angles and fullfill the corresponding sampling requirements. Overall, it is even a bit amazing that the found projection method could well compete with the BFGMRES solver, which needs considerably more computer memory and also slightly more computation time per iteration due to the orthogonalization of a considerably larger search space.

## References


[1] S. Rao, D. Wilton, and A. Glisson, "Electromagnetic scattering by surfaces of arbitrary shape," *IEEE Transactions on Antennas and Propagation*, vol. 30, no. 3, pp. 409–418, May 1982.

[2] W. C. Chew, J.-M. Jin, E. Michielssen, and J. Song, *Fast and Efficient Algorithms in Computational Electromagnetics*. Boston: Artech House.

[3] H. Guo, Y. Liu, J. Hu, and E. Michielssen, "A butterfly-based direct integral-equation solver using hierarchical lu factorization for analyzing scattering from electrically large conducting objects," *IEEE Transactions on Antennas and Propagation*, vol. 65, no. 9, pp. 4742–4750, Sep. 2017.

[4] M. H. Gutknecht, "Block Krylov space methods for linear systems with multiple right-hand sides: An introduction," 2006.

[5] P. Fischer, "Projection techniques for iterative solution of ax=b with successive right-hand sides," *Elsevier Computer Methods in Applied Mechanics and Engineering*, vol. 163, pp. 193–204, 09 1998.

[6] Y. Saad, "A flexible inner-outer preconditioned GMRES algorithm," *SIAM Journal on Scientific Computing*, vol. 14, no. 2, pp. 461–469, 1993.

[7] I. V. Lindell, "Huygens' principle in electromagnetics," *IEE Proceedings - Science, Measurement and Technology*, vol. 143, no. 2, pp. 103–105, March 1996.

[8] T. F. Eibert, "Some scattering results computed by surface-integral-equation and hybrid finite-element - boundary-integral techniques, accelerated by the multilevel fast multipole method," *IEEE Antennas and Propagation Magazine*, vol. 49, no. 2, pp. 61–69, April 2007.

[9] M. H. Gutknecht and T. Schmelzer, "The block grade of a block Krylov space," *Linear Algebra and its Applications*, vol. 430, no. 1, pp. 174 – 185, 2009.

[10] J. Hansen, *Spherical Near-field Antenna Measurements*, ser. IET Electromagnetic Waves Series. London, UK: IET, 2008.

[11] Y. Saad, *Iterative Methods for Sparse Linear Systems*, 2nd ed. Philadelphia, PA, USA: Society for Industrial and Applied Mathematics, 2003.